Environmental Science & Technology

pubs.acs.org/est

Article

Unique On-Site Spinning Sampling of Highly Water-Soluble Organics Using Functionalized Monolithic Sorbents

Junlang Qiu, Caley B. Craven, Nicholas J. P. Wawryk, Gangfeng Ouyang, and Xing-Fang Li*

Cite This: *Environ. Sci. Technol.* 2022, 56, 8094−8102

Read Online

ACCESS | Metrics & More | Article Recommendations | Supporting Information

ABSTRACT: Water utilities encounter unpredictable odor issues that cannot be explained by routine water parameters during spring runoff, even in the summer and fall. Highly water-soluble organics (*e.g.*, amino acids and saccharides) have been reported to form odorous disinfection byproducts during disinfection, but the lack of simple and practical on-site sampling techniques hampers their routine monitoring at trace levels in source water. Therefore, we have created two functionalized nested-in-sponge silica monoliths (NiS-SMs) using a one-pot synthesis method and demonstrated their application for extracting highly soluble organics in water. The NiS-SMs functionalized with the sulfonic group and phenylboronic moiety selectively extracted amino acids and monosaccharides, respectively. We further developed a spinning sampling technique using the composites and evaluated its robust performance under varying water conditions. The spinning sampling coupled to high-performance liquid chromatography tandem mass spectrometry analysis provided limits of detection for amino acids at 0.038−0.092 ng L^{-1} and monosaccharides at 0.036−0.14 ng L^{-1}. Using the pre-equilibrium sampling-rate calibration, we demonstrated the applicability of the spinning sampling technique for on-site sampling and monitoring of amino acids and monosaccharides in river water. The new composite materials and rapid on-site sampling technique are unique and efficient tools for monitoring highly soluble organics in water sources.

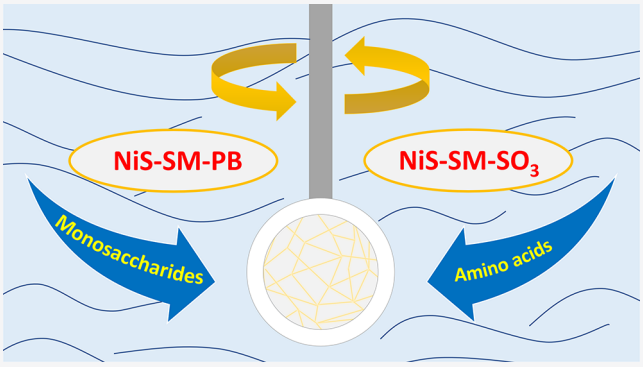

KEYWORDS: *on-site, spinning sampling, water-soluble organics, nested-in-sponge silica monolith, water monitoring*

INTRODUCTION

Water utilities are encountering unpredictable odor issues which cannot be fully explained by routine water parameters such as turbidity, dissolved organic carbon (DOC), and dissolved organic nitrogen (DON). Natural biological matter pervasively degrades to soluble organics in surface water,[1−4] some of which have been recognized as precursors of odorous drinking water disinfection byproducts (DBPs).[5−7] Among the numerous natural organics in the water environment, previous studies tended to focus on large molecules such as peptides.[8−10] However, most of the large peptides are effectively removed by coagulation and/or filtration before disinfection,[11] and the remaining peptides break down to small peptides or even amino acids.[12] Amino acids are ubiquitous in source water and can react with disinfectants to produce odorous, off-taste, and toxic DBPs.[13−15] Additionally, natural carbonaceous matter may impact the drinking water quality including odor/off-taste issues.[16,17] Polysaccharides represent a class of important natural carbonaceous matter in water that can readily break down to monosaccharides and form DBPs.[16] Therefore, exploring the presence of both amino acids and monosaccharides in water is important to understand their roles in drinking water odor/off-taste issues.

Monitoring organics in water is important in water research.[18,19] On-site sampling is a promising tool for obtaining environmental information because of its ability to eliminate the collection, transport, and storage of large volumes of water samples.[20] An ideal on-site sampling method should be convenient, inexpensive, rapid, sensitive, and robust for field application. Recent developments in passive and active sampling methods have shown significant improvement. However, their applications in field studies remain challenging, and in particular, their application for monitoring soluble organics in water is scarce.[21−23] Passive sampling enrichment of organic contaminants is easily influenced by hydrodynamic and chemical conditions of the field (*e.g.*, water turbulence, water pH, temperature, and fouling/biofouling).[24−27] Active sampling methods require intricate and expensive assembling.[28−32] The on-site sampling of highly soluble organics in

Received: February 17, 2022
Revised: May 11, 2022
Accepted: May 12, 2022
Published: May 27, 2022

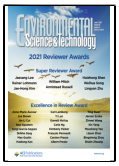

https://doi.org/10.1021/acs.est.2c01202
Environ. Sci. Technol. 2022, 56, 8094−8102

source waters has not been well studied because of the high solubility of organics, as well as their high polarity and occurrence at low concentrations, which creates additional difficulties.[33,34] The lack of simple and practical on-site sampling techniques hampers routine quantitative monitoring of trace-level highly soluble organics in source water from creeks, rivers, and lakes. Therefore, we aimed to develop new materials and an on-site sampling method to address these difficulties in this study.

Using a silica monolith (SM) as the material for on-site sampling has several advantages including uniform interconnected pores, a large surface area, and an easily functionalized surface.[35−37] This versatile material has been widely used in the capillary chromatographic stationary phase but its use in solid-phase extraction (SPE) has been limited due to its brittleness.[38,39] To solve this problem, we introduced a nested-in-sponge SM (NiS-SM) composite in a previous study.[40] Because of the nested sponge skeleton, the NiS-SM material has enhanced mechanical flexibility, enabling the creation of desirable shapes using the NiS-SM material for specific applications. Moreover, the tunable surface chemistry of the SM allows for various functionalizations of the NiS-SM in separate steps.[37,41−44] In addition to its superior performance, preparation of the NiS-SM is simple and cost-effective. Herein, we propose to simplify the synthesis and functionalization of the NiS-SM in a single pot to maximize its applications for water monitoring.

To demonstrate the application of the functionalized NiS-SM for monitoring highly soluble organics, we created a new functionalized NiS-SM that specifically enriches amino acids and monosaccharides in source water. The functionalized NiS-SM composites were synthesized *via* a simple and convenient one-pot strategy and shaped into thin disks. We also developed and validated a spinning sampling method for extraction of amino acids and monosaccharides in both laboratory and field settings. This study provides a new one-pot synthesis method for a functionalized NiS-SM and demonstrates unique on-site sampling of highly soluble organics through the analysis of amino acids and monosaccharides in river water.

METHODS AND MATERIALS

Chemicals and Materials. Tetramethoxysilane (TMOS), vinyltrimethoxysilane (VTMS), urea, polyethylene glycol (PEG, M_n = 10,000), 4-vinylphenylboronic acid (VPBA), 4-vinylphenylsulfonic acid sodium salt (VPSA), α,α'-azoisobutyronitrile (AIBN), 1-phenyl-3-methyl-5-pyrazolone (PMP), formic acid, ammonium acetate, 1-butanol (containing 3 M hydrogen chloride), standards of monosaccharides [D-ribose (Rib), 2-deoxy-D-ribose (Deo), L-rhamnose (Rha), D-mannose (Man), D-glucose (Glu), D-galactose (Gal), and D-fructose (Fru)] and amino acids [L-asparagine (Asp), L-proline (Pro), L-valine (Val), L-glutamine (Gln), L-tyrosine (Tyr), L-methionine (Met), and L-phenylalanine (Phe)], and a deuterated standard (D-glu-$^{13}C_6$) were purchased from Sigma-Aldrich (St. Louis, MO). The other three deuterated standards (L-val-d_1, L-val-d_8, and D-glu-d_2) were purchased from C/D/N isotopes (Pointe-Claire, Quebec, Canada). Optima water, methanol, acetic acid, chloroform, diethylene glycol, and acetonitrile were purchased from Fisher Scientific (Fair Lawn, NJ). Oasis MCX cartridges (6 cc, 150 mg) were purchased from Waters (Milford, MA). Empty syringe cartridges (60 mL) were purchased from Agilent Technologies (Santa Clara, CA). The melamine−formaldehyde sponges (RioRand) were purchased from Amazon.

Preparation and Functionalization of NiS-SM. The NiS-SM was prepared as detailed in our previous study, with the incorporation of two functional monomers, VPSA and VPBA.[40] Briefly, TMOS (10.8 mL), VTMS (3.6 mL), and PEG (3.0 g) were added to an aqueous acetic acid solution (0.01 M, 30 mL). The mixture was stirred in an ice-water bath for 1 h. Next, VPBA (2.0 g) and AIBN (20 mg, in 2.0 mL of diethylene glycol) were added to the mixture. The mixture was stirred for 10 min and then sonicated for an additional 10 min. Subsequently, the mixture was absorbed by a sponge, and the saturated sponge was maintained at 55 °C for 12 h followed by 80 °C for 8 h. The resulting NiS-SM-PB was washed thoroughly with water and shaped into thin disks (diameter 27 mm, thickness 3 mm). The preparation of NiS-SM-SO_3 followed the same procedure with VPBA changed to VPSA (3.0 g).

Characterization of New Composite Materials. The morphology of the NiS-SM composites was characterized on a Zeiss EVO M10 scanning electron microscope (Zeiss, Oberkochen, Germany). The functionalization was characterized using a Nicolet iS50 Fourier transform infrared (FT-IR) spectrometer with an attenuated total reflection (ATR) mode (Thermo Fisher Scientific, Waltham, MA) and a Kratos AXIS Ultra X-ray photoelectron spectroscope (Kratos Analytical, Manchester, UK).

Extraction and Desorption. A functionalized NiS-SM disk was packed in a sampling tool (customized in the mechanical shop at the University of Alberta), and the device was mounted on a rotary tool (RZR 2021, Heidolph) for spinning sampling (Figure S1). Before extraction, the NiS-SM-SO_3 disk was saturated with acidic aqueous solution (FA, 0.5%, v/v), while the NiS-SM-PB disk was saturated with Optima water. Next, the device was immersed into water vertically to a depth of approximately 10 cm with the rotary tool switched on to start sampling.

After sampling, the disk was removed from the device and packed in an empty cartridge for elution (Figure S1). Prior to elution, the disk was dried by a vacuum air stream. (a) For the NiS-SM-SO_3 disk, the amino acids were eluted with 10 mL of methanolic solution (ammonium hydroxide, 1 wt %). After the surrogate Val-d_1 (10 μL, 10 ng mL^{-1}) was added, the eluent was derivatized and then reconstituted in 100 μL of Optima water. The reconstituted solution was passed through a syringe filter, and the internal standard butyl-Val-d_8 (10 μL, 10 ng mL^{-1}) was added before instrument analysis. (b) For the NiS-SM-PB disk, the monosaccharides were eluted with 10 mL of aqueous solution (acetic acid, 0.1 M). After the surrogate Glu-d_2 (10 μL, 10 ng mL^{-1}) was added, the eluent was derivatized and then concentrated to 100 μL of aqueous solution. The solution was passed through a syringe filter, and the internal standard PMP-Glu-$^{13}C_6$ (10 μL, 10 ng mL^{-1}) was added before instrument analysis. Details on the derivatization methods are described in the Supporting Information (Text S1).

Evaluation of Extraction Performance. The extraction kinetic profiles for amino acids and monosaccharides were evaluated. The spiking concentration of each analyte in deionized water (pH 7) was 10 ng L^{-1}, and the spiking water was static and maintained at 20 °C. The spinning rate was 1000 rpm, and the durations of sampling were 1, 2, 4, 6, 8, 10, 12, 30, and 60 min. The first-order kinetics model was

https://doi.org/10.1021/acs.est.2c01202
Environ. Sci. Technol. 2022, 56, 8094−8102

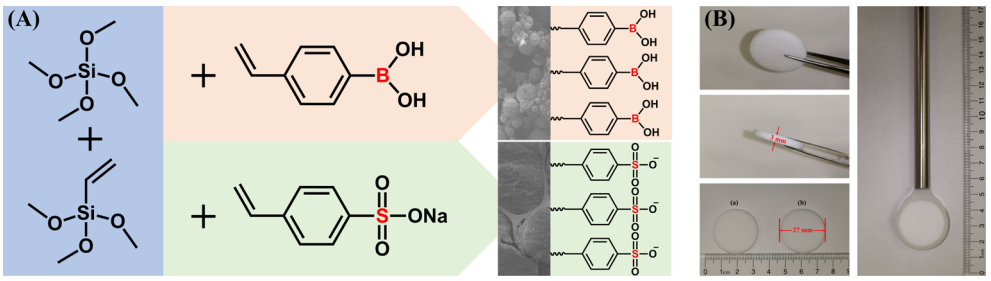

Figure 1. (A) Schematic illustration of synthesis and functionalization of the NiS-SM materials. (B) Photographs of the functionalized NiS-SM disks [(a) NiS-SM-SO_3 and (b) NiS-SM-PB] and the customized sampling device packed with a NiS-SM disk.

utilized to fit the extracted amounts on the disk and the extraction durations

$$n = n_e \cdot (1 - \exp(-k_{ex} \cdot t)) \quad (1)$$

where t is the extraction duration, n is the extracted amount of the analyte on the disk at t, n_e is the equilibrium extracted amount, and k_{ex} is the extraction rate constant.

The impacts of water temperature, water pH, and water turbulence on the extraction performance were evaluated. The reference conditions were: static water, water pH 7, water temperature 20 °C, spinning rate 1000 rpm, and spiking concentration 10 ng L^{-1} each. For the field implementation, the evaluation conditions were set as follows: (a) for water temperature evaluation, the temperature was maintained at 10 and 30 °C, respectively; (b) for water pH evaluation, the water pH was adjusted to 6 and 8, respectively; and (c) for water turbulence evaluation, the simulated linear water flow rate was set at 0.2 and 0.4 m s^{-1}, respectively.

Calibration. The analyte concentration in water was quantified by the pre-equilibrium sampling-rate calibration.[23] The relationship between the concentration of the analyte in water and the extracted amount of the analyte on the disk can be expressed as

$$n = R_s C_s t \quad (2)$$

where n is the extracted amount of the analyte on the disk, C_s is the concentration of the analyte in water, R_s is the sampling rate for the analyte, and t is the sampling duration. The sampling rates are required for quantification. To determine the sampling rates, the sampling durations were set at 1, 2, 4, 6, 8, 10, and 12 min. The sampling rate was calculated by fitting the peak areas and the sampling durations to the linear equation ($y = kx$). For the field application, the analyte concentrations in water were calculated based on eq 2 using the acquired sampling rates.

The analytical merits, reproducibility, sensitivity, and linearity, were evaluated. The extraction conditions were: static water, water pH 7, water temperature 20 °C, spinning rate 1000 rpm, and sampling duration 5 min. The inter-reproducibility was evaluated by spiking water samples at 1 and 100 ng L^{-1}. The sensitivity, including the method detection limit (MDL) and the method quantification limit (MQL), was evaluated in spiked water samples and calculated as the signal-to-noise (S/N) ratio at 3 (MDL) and 10 (MQL), respectively. The linearity was evaluated by fitting the peak areas and the spiking concentrations to the linear equation.

Field Application. Field trials were performed in the North Saskatchewan River, with the sampling location about 1 m distance from the shore (Figure S2). A portable hand drill (DCD777C2, DEWALT) was used for on-site spinning sampling. During sampling, the device was immersed vertically into river water to a depth of approximately 10 cm. The sampling duration was 5 min, and the spinning rate was 1000 rpm. After sampling, the disks were transported to the laboratory for analysis. At the same time, river water was collected by grab sampling at the same sampling location and transported to the laboratory for a comparative study. The concentration of amino acids and monosaccharides in collected river water was determined by conventional preparation methods coupled to high-performance liquid chromatography tandem mass spectrometry (HPLC−MS/MS) analysis. The grab sampling and conventional preparation methods are described in detail in the Supporting Information (Text S2).

HPLC−MS/MS Analysis. Instrument analysis was performed on an Agilent 1290 series HPLC system coupled to a Sciex QTRAP 5500 triple-quadrupole ion-trap MS/MS system. Instrument control and data collection were performed using Analyst software (version 1.5.2, AB SCIEX, Framingham, MA). The instrument analysis is described in detail in the Supporting Information (Text S3).

Quality Assurance and Quantity Control. Each sample was examined in triplicate from the spinning sampling to HPLC−MS/MS analysis. Blank controls were obtained in parallel by spinning sampling of blank deionized water using both NiS-SM-SO_3 and NiS-SM-PB disks. None of the target analytes were detected in the blank controls, confirming that the analytes detected in laboratory experiments and field applications were from the spiked water and river water, respectively. The surrogate standards Val-d_1 or Glu-d_2 were added to the eluents to confirm the recoveries. The internal standards butyl-Val-d_8 or PMP-Glu-$^{13}C_6$ were added before the instrument analysis to account for the potential variations in the instrument response and matrix-induced signal bias in ionization. Each of the targeted analytes was confirmed based on multiple reaction monitoring (MRM) ion transitions and the retention time of its authentic standard. Analytes from the HPLC−MS/MS analysis were quantified by internal standard calibration using the internal deuterated standards. Statistical comparison was performed using the t-test with a P-value lower than 0.05 indicating statistical significance.

RESULTS AND DISCUSSION

One-Pot Preparation and Characterization of Functionalized NiS-SMs. Figure 1 shows (A) the synthesis and functionalization of NiS-SM-SO_3 and NiS-SM-PB *via* a one-pot strategy and (B) photographs of the prepared SPE disks. The new one-pot strategy is both simple and practical, eliminating the multiple steps of synthesis and functionalization of the previous approach.[40] The one-pot method incorporated the organic functional monomers in the siloxane

https://doi.org/10.1021/acs.est.2c01202
Environ. Sci. Technol. 2022, 56, 8094−8102

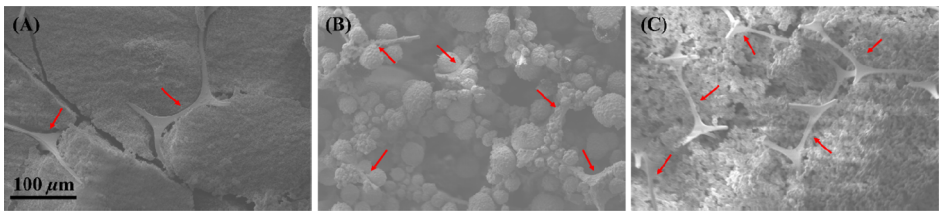

Figure 2. SEM images of NiS-SM-SO_3 (A), NiS-SM-PB (B), and unmodified NiS-SM (C). The scale bar applies to all of the images. The sponge skeleton is marked by arrows.

matrix to allow for simultaneous synthesis and functionalization. Briefly, a piece of sponge was soaked in a mixture solution of hydrolyzed alkoxysilanes and a functional organic monomer in an ice bath. Subsequently, gel formation involving the vinyl-containing monomer occurred *in situ* within the sponge pores. We took advantage of specific chemical interactions to create the selectivity of the functionalized NiS-SM for amino acids and monosaccharides. Selective extraction of monosaccharides was facilitated by the interactions between the phenyl boronic moiety of VPBA and the *cis*-diol moieties of the monosaccharides,[45,46] while amino acid selectivity was facilitated through the interactions between the sulfonate group of VPSA and the free amine groups of the amino acids.[40] Additionally, the benzene rings of the functional monomers and the siloxane matrix have extraction affinity for the lipophilic moieties of the targeted analytes. It is important to note that in aqueous solution, deoxyribose predominantly exists in the six-membered ring structure of a *cis*-diol moiety; therefore, the PB functionalization has strong affinity for deoxyribose in water.

The characteristics of functionalized NiS-SM-PB and NiS-SM-SO_3 compared to the unmodified NiS-SM were examined using scanning electron microscopy (SEM), X-ray photoelectron spectroscopy (XPS), and FT-IR spectroscopy. Figure 2 shows the SEM images of (A) NiS-SM-SO_3, (B) NiS-SM-PB, and (C) unmodified NiS-SM. As expected, the morphological characteristics significantly changed after the functional organic monomers were incorporated. Compared to the unmodified NiS-SM (Figure 2A), the incorporation of VPSA and VPBA monomers densified the SM (Figure 2B,C, respectively). The densification enhanced the adhesion of the SM materials to the sponge skeleton, providing functionality for various interactions. Incorporation of the VPBA monomer resulted in congregation of the silica particles on the skeleton. NiS-SM-PB had an interconnected macroporous structure favorable for mass transfer within the composite, while the more compact structure of NiS-SM-SO_3 had a larger extraction capacity. The element distributions of the composites were mapped using SEM-energy-dispersive X-ray mapping analysis (Figure S3). The silicon signal and the nitrogen signal were derived from the SM and the sponge skeleton, respectively, while the distributions of sulfur and boron indicated the incorporation of the VPSA monomer and the VPBA monomer, respectively. The XPS analysis further confirmed the presence of the specific elements on the surfaces of the composites, that is, S 2p in NiS-SM-SO_3 and B 1s in NiS-SM-PB (Figure S4). Additionally, the characteristic peaks of FT-IR analysis demonstrated the incorporation of the phenyl boronic moiety (633, 651, 754, and 1609 cm^{-1}) and the phenyl sulfonic moiety (970, 1052, and 1622 cm^{-1}) (Figure S5). These results confirmed the successful preparation of NiS-SM-SO_3 and NiS-SM-PB *via* an efficient and convenient one-pot strategy.

The unique physical and mechanical features of NiS-SM-SO_3 and NiS-SM-PB enabled the creation of the large SPE disks (Figure 1B) while overcoming the brittleness of the SM. Because of its nested sponge skeleton, the NiS-SM has a unique reinforced concrete structure and great mechanical flexibility. The bulk NiS-SM-SO_3 and NiS-SM-PB were shaped into cylinders with a diameter of 27.0 mm using a hole punch, and the cylinders were sliced into thin disks with a thickness of 3.0 mm (Figure 1B). The NiS-SM-SO_3 disk weights were 513−552 mg (average 531 mg) and the NiS-SM-PB disk weights were 478−514 mg (average 503 mg). A disk was packed in a custom-made sampling device mounted on a rotary tool for spinning sampling (Figure 1B). The SM materials swell slightly when saturated with aqueous solution; therefore, the disk can be held tightly on the sampling device during spinning sampling (at the set rate, 1000 rpm). Herein, we developed a new one-pot preparation method to create SPE cartridges in the laboratory. This simple and efficient strategy allowed us to create different and new functional materials easily for environmental analysis of a wide range of organic compounds.

Development of the Spinning Sampling Method. Extraction of highly soluble organics in water is challenging. To address this issue, we used the SPE disks made of NiS-SM-SO_3 and NiS-SM-PB to develop a spinning sampling method for the analysis of highly water-soluble organic compounds in water using amino acids and monosaccharides as examples. We first examined the extraction kinetics to establish the spinning sampling method. We anticipated utilizing the spinning power to accelerate the extraction mass transfer. However, as shown in Figure S6, the extraction kinetics for both amino acids and monosaccharides did not reach equilibrium after 60 min. The first-order kinetics modeling results indicated that the predicted equilibrium times of the analytes were much longer than 60 min. The long extraction equilibrium time may be due to the significantly larger extraction phase volume of the disks compared to the tiny coating volumes of common solid-phase microextraction (SPME) fibers. At 60 min, the extracted amounts of amino acids were approximately 10 times larger than those of monosaccharides. The chemical properties of different functionalized surfaces could be a reason for the difference in extracted amounts. The functionalization with the phenyl sulfonic moiety for amino acids was based on the anion−cation ($-SO_3^-$ and $-NH_3^+$) interaction, while the functionalization with the phenyl boronic moiety for monosaccharides was based on the covalent complex formation between the phenyl boronic moiety and *cis*-diol. Compared to the covalent complex formation resulting from the sharing of an electron pair between atoms, the noncovalent electrostatic attraction requires less stringent conditions and is thus more efficient. Therefore, the extraction affinity of NiS-SM-SO_3 for amino acids was stronger and the extracted

https://doi.org/10.1021/acs.est.2c01202
Environ. Sci. Technol. 2022, 56, 8094−8102

Table 1. Analytical Merits of the Spinning Sampling Technique Coupled to HPLC−MS/MS Analysis for the Amino Acids and Monosaccharides[a]

analyte		LOD (ng mL^{-1})	LOQ (ng mL^{-1})	MDL (ng L^{-1})	MQL (ng L^{-1})	linearity		inter-reproducibility (RSD, n = 3, %)	
						range (ng L^{-1})	R^2	1 ng L^{-1}	100 ng L^{-1}
amino acids	Asp	0.054	0.18	0.077	0.26	1−100	0.9993	16.8	11.7
	Gln	0.10	0.34	0.078	0.26	0.5−100	0.9993	9.4	11.9
	Met	0.086	0.29	0.092	0.31	0.5−100	0.9968	4.3	5.5
	Phe	0.033	0.11	0.066	0.22	0.5−100	0.9986	2.3	3.1
	Pro	0.046	0.15	0.038	0.13	0.5−100	0.9996	3.6	10.0
	Tyr	0.067	0.22	0.066	0.22	0.5−100	0.9998	2.8	6.6
	Val	0.051	0.17	0.056	0.19	1−100	0.9989	8.9	5.9
monosaccharides	Deo	0.0016	0.0053	0.036	0.12	0.5−100	0.9993	16.9	5.5
	Gal	0.0013	0.0044	0.049	0.16	0.5−100	0.9951	3.6	7.8
	Glu	0.00077	0.0026	0.054	0.18	0.5−100	0.9949	6.1	5.5
	Man	0.0021	0.0070	0.14	0.47	0.5−100	0.9950	3.2	8.2
	Rha	0.0012	0.0040	0.045	0.15	0.5−100	0.9949	3.8	3.9
	Rib	0.0012	0.0039	0.059	0.20	0.5−100	0.9954	6.6	6.7
	Xyl	0.00094	0.0031	0.036	0.12	0.5−100	0.9931	5.5	4.6

[a]Note that the amino acids and monosaccharides were derivatized before instrument analysis.

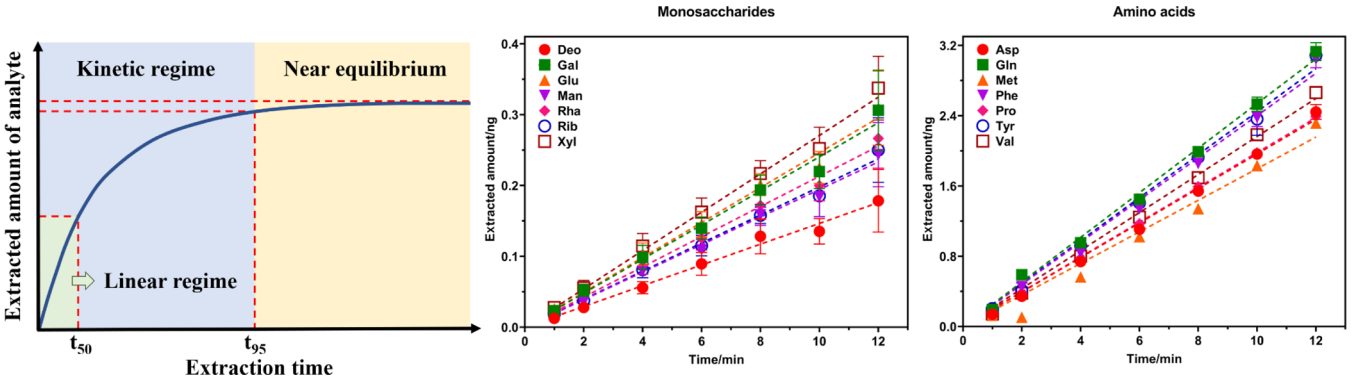

Figure 3. Theoretical extraction profile and extraction kinetics of the monosaccharides and the amino acids within 12 min. The concentration for each of the amino acids and monosaccharides in water was 10 ng L^{-1}. Error bars represent SDs of triplicates.

amounts of the amino acids were larger. Considering that capturing the extremely polar and hydrophilic monosaccharides in water is very challenging, the extraction performance of NiS-SM-PB for monosaccharides has an MDL ranging 0.036−0.14 ng L^{-1} when coupled to HPLC−MS/MS analysis (Table 1). This demonstrates the applicability of NiS-SM-PB for the analysis of monosaccharides.

Figure 3 presents a theoretical sampling kinetic profile: the extracted amount of the analytes on the extraction phase corresponding to the extraction time.[47] t_{50} and t_{95} are the extraction times when the extracted amounts reach 50 and 95% of the equilibrium extraction amount, respectively. The theoretical extraction can be divided into two regimes: time 0 to t_{95}, kinetic regime; after t_{95}, near-equilibrium regime. When the extraction time is shorter than t_{50}, the extraction kinetics process is close to linear. Calibration of analyte concentration is based on the extraction process in either the equilibrium regime or the kinetic regime.[47] In this study, the slow extraction equilibrium of the spinning sampling indicated that equilibrium calibration was not suitable. Consequently, the calibration of the spinning sampling method was based on the kinetic extraction process.

In the initial phase of extraction, desorption of an analyte from the extraction phase to water can be negligible; therefore, the load of the analyte is directly proportional to its bulk concentration in water.[48,49] In other words, when the extraction time is shorter than t_{50}, the extraction kinetics process is linear. When rapid extraction happens in the linear regime, the extraction process can be described by eq 2. The sampling rate is defined as a proportionality constant, interpreted as the volume of water cleared of targeted analyte per unit of sampling duration by the extraction phase. In this study, we measured the extracted amounts at 1, 2, 4, 6, 8, 10, and 12 min and fitted the results to the linear equation ($y = kx$). For the two classes of analytes (amino acids and monosaccharides), good linear correlation coefficients were achieved (Figure 3). The coefficients for amino acids ranged from 0.9892 to 0.9999 and for monosaccharides from 0.9963 to 0.9982, indicating that within 12 min, the extraction process of the spinning sampling method followed the linear mass uptake. According to eq 2, the slope (k) of the linear correlation is equal to the product of the analyte concentration in water (C_s) and the sampling rate (R_s). As a result, the sampling rates were calculated to be 18.0 to 25.4 mL min^{-1} for amino acids and 1.8 to 2.7 mL min^{-1} for monosaccharides (Table S1). Similar to the extracted amounts, the sampling rates for amino acids were approximately 10 times higher than those for monosaccharides, which could be attributed to the difference in extraction efficiency between NiS-SM-SO_3 and NiS-SM-PB. In field applications, when the extracted amounts

https://doi.org/10.1021/acs.est.2c01202
Environ. Sci. Technol. 2022, 56, 8094−8102

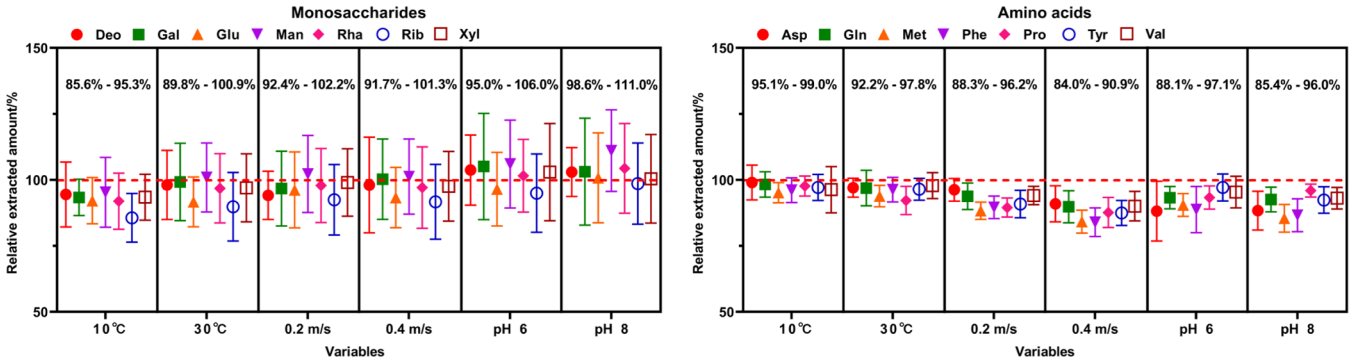

Figure 4. Relative extracted amounts obtained under the specified variable conditions (water temperature at 10 or 30 °C, simulated linear water flow rate at 0.2 or 0.4 m s^{-1}, and water pH at 6 or 8). The relative extracted amounts were calculated by comparing them to the average extracted amounts under the reference conditions (static water, water temperature 20 °C, and water pH 7). Error bars represent SDs of triplicates.

on the extraction phase corresponding to a designated sampling duration (within 12 min) are measured, the analyte concentrations in water can be determined using the acquired sampling rates based on eq 2.

Evaluation of the Spinning Sampling Method. When the thin disk is spinning around the axis of the shaft vertically in water, the mass transfer is associated with the relative motion of the disk and water. Since the mathematics of mass diffusion and heat diffusion described by Laplace's equation are equivalent, the formula for heat transfer can be adapted for mass transfer by substituting thermal conductivity and diffusivity constants with mass diffusion coefficients.[50,51] Therefore, the mass transfer of spinning extraction is associated with the following parameters[52]

$$n = f_1(\mathrm{Re},\ \mathrm{Pr},\ D,\ d,\ A,\ C_w,\ t) \tag{3}$$

where *Re* is the Reynolds number, *Pr* is the Prandtl number, *D* is the diffusion coefficient, *d* is the disk thickness, *A* is the disk top/bottom surface area, C_w is the analyte concentration in water, and *t* is the extraction duration. For a designated extraction process, eq 3 can be simplified as

$$n = f_2(\mathrm{Re},\ \mathrm{Pr},\ D) \tag{4}$$

In practice, *Re*, *Pr*, and *D* depend mainly on the spinning rate (*S*), water turbulence (*W*), and water temperature (*T*), so eq 4 can be substituted as

$$n = f_3(S,\ W,\ T) \tag{5}$$

Additionally, the water pH may influence the mass transfer because the amino acids and the monosaccharides are ionizable in water. Consequently, to validate the spinning sampling method, we evaluated variables comprising the spinning rate, water turbulence, water temperature, and water pH.

Theoretically, increasing the spinning rate can accelerate the mass transfer and improve the extraction efficiency. However, to ensure the robust operation of sampling, we had to choose a practical and steady spinning rate to avoid losing the disk or even collapse of the sampling device. Therefore, the spinning rate was set at 1000 rpm. The other variables, the water temperature, water pH, and water turbulence, were evaluated in the laboratory setting. An initial set of conditions (static water, 20 °C, and pH 7) was used as reference for evaluation of the variables. We examined the effect of one parameter at a time, while the other conditions remained unchanged. The extracted amounts were compared to those obtained under the reference conditions. As shown in Figure 4, the extraction performance for the monosaccharides and amino acids remained stable when the variables changed within the specific range tested. The impact of water turbulence was found to be negligible when the water flow rate was lower than 0.4 m s^{-1}. No significant variation of the extraction performance was observed when the water temperature was changed to 10 and 30 °C and the water pH was changed to 6 and 8. For common passive samplers that are exposed directly in water (*e.g.*, film-based samplers), water conditions can have significant influence on their extraction performance and result in uncertainty in determination. In this study, the spinning enhancement endowed the technique with resistance to water conditions and minimized the impacts of the variables on the extraction performance. In short, the spinning sampling technique was able to maintain steady sampling performance when the major variables were changed within certain ranges.

Analytical Merits. According to the linear process of the extraction kinetics, the sampling duration was set at 5 min for the two classes of analytes for the best sampling speed, efficiency, and sensitivity. Table 1 summarizes the analytical values of the spinning sampling, showing excellent reproducibility and sensitivity for the two classes of analytes. The relative standard deviations (RSDs) for the amino acids ranged from 2.3 to 16.8% at 1 ng L^{-1} and 3.1 to 11.9% at 100 ng L^{-1}, while the RSDs were 3.2 to 16.9% at 1 ng L^{-1} and 3.9 to 8.2% at 100 ng L^{-1} for the monosaccharides. The MDLs and MQLs were 0.038 to 0.092 ng L^{-1} and 0.13 to 0.31 ng L^{-1} for the amino acids and 0.036 to 0.14 ng L^{-1} and 0.12 to 0.47 ng L^{-1} for the monosaccharides, respectively. The excellent method sensitivity demonstrated that the spinning sampling technique was capable of capturing trace-level analytes in environmental water. Additionally, the linear range was 0.5−100 ng L^{-1} for the amino acids Gln, Met, Phe, Pro, and Tyr with R^2 ranging from 0.9968 to 0.9998 and 1.0−100 ng L^{-1} for the amino acids Asp and Val with R^2 at 0.9993 and 0.9989. For the monosaccharides, the linear range was 0.5−100 ng L^{-1} with R^2 ranging from 0.9931 to 0.9993. Note that the linear range top limit was tested at 100 ng L^{-1} considering the realistic requirements of the field trial in river water. However, owing to the excellent extraction performance of the functionalized NiS-SM materials and the large extraction phase volume, the inherent linear range top limit can be much higher than 100 ng L^{-1}.

On-Site Sampling and Monitoring. Having established the spinning sampling technique in the laboratory setting, we

https://doi.org/10.1021/acs.est.2c01202
Environ. Sci. Technol. 2022, 56, 8094−8102

Table 2. Determination Results (ng L^{-1}) Derived from Grab Sampling and On-Site Spinning Sampling[a]

analyte		grab sampling				spinning sampling				comparison
		I	II	III	mean ± SD	I	II	III	mean ± SD	
amino acids	Asp	1.4	1.6	0.9	1.3 ± 0.36	2.5	2.8	3.4	2.9 ± 0.46	ns
	Gln	3.9	3.6	3.1	3.5 ± 0.40	7.6	5.3	6.4	6.4 ± 1.2	*
	Met	2.0	3.3	2.0	2.4 ± 0.75	3.5	3.1	4.3	3.6 ± 0.61	ns
	Phe	23	42	20	28 ± 12	24	20	19	21 ± 2.6	ns
	Pro	6.7	9.0	5.5	7.1 ± 1.8	8.1	11	12	10 ± 2.0	ns
	Tyr	15	34	15	21 ± 11	17	21	14	17 ± 3.5	ns
	Val	5.7	9.8	5.3	6.9 ± 2.5	7.8	6.6	9.5	8.0 ± 1.5	ns
monosaccharides	Deo	0.8	1.2	1.0	1.0 ± 0.2	4.3	1.1	2.0	2.5 ± 1.7	ns
	Gal	17	23	15	18 ± 4.2	14	13	8.6	12 ± 2.9	ns
	Glu	38	35	38	37 ± 1.7	66	91	52	70 ± 20	ns
	Man	16	20	19	18 ± 4.2	15	13	9.7	13 ± 2.7	ns
	Rha	8.0	8.5	6.7	7.7 ± 0.93	7.9	6.5	4.4	6.3 ± 1.8	ns
	Rib	59	57	72	63 ± 8.1	15	11	9.2	12 ± 3.0	*
	Xyl	20	17	18	18 ± 1.5	24	27	16	22 ± 5.7	ns

[a]*denotes significant difference ($P < 0.05$) and ns denotes no significant difference.

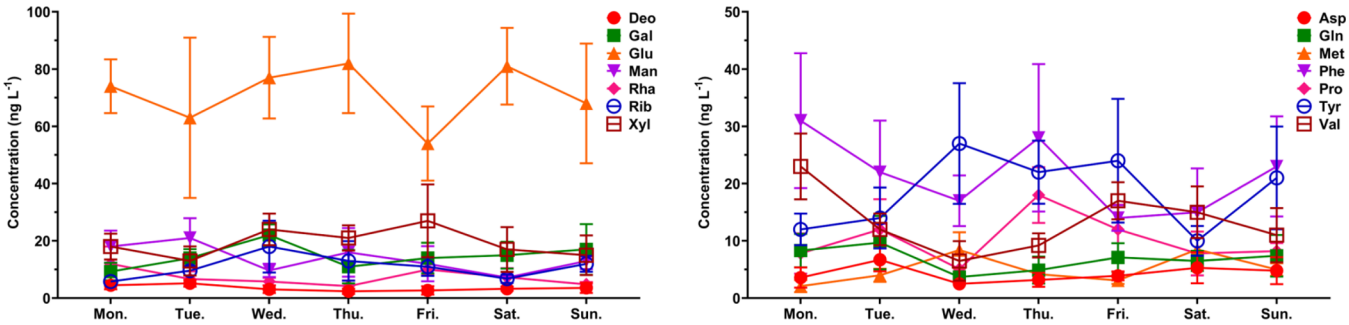

Figure 5. Monitoring of the monosaccharides and amino acids in river water using the on-site spinning sampling technique over a week. Error bars represent SDs of triplicates.

subsequently demonstrated it in a field trial. The North Saskatchewan River is the source water for drinking water for a population of over a million; thus, it was chosen for the on-site field trial. The river water conditions were: water temperature 21 °C, water flow rate <0.3 m s^{-1}, and water pH 6.9. Triplicate samples were collected in parallel by spinning sampling and grab sampling at the same location. Table 2 presents the concentrations of the amino acids and monosaccharides determined in the spinning sampling and grab sampling samples. The two approaches provided consistent results. For the spinning sampling, the amino acid concentrations ranged from 2.9 ng L^{-1} (Asp) to 21 ng L^{-1} (Phe) and the monosaccharide concentrations ranged from 2.5 ng L^{-1} (Deo) to 70 ng L^{-1} (Glu). For the grab sampling, the amino acid concentrations ranged from 1.3 ng L^{-1} (Asp) to 28 ng L^{-1} (Phe) and the monosaccharide concentrations ranged from 1.0 ng L^{-1} (Deo) to 63 ng L^{-1} (Rib). The two groups of concentrations were examined by a two-tailed Student's *t*-test to statistically evaluate the significance of the differences. No statistically significant difference was observed for any analyte except for one amino acid (Gln) and one monosaccharide (Rib). According to the theory of sampling-rate calibration, the calibration is independent of the water volume when the water volume is much larger than the extraction phase volume. In the kinetic linear regime, the mass load of the analyte is in direct proportion to the bulk analyte concentration in water. For on-site sampling, the water volume related to bulk concentrations is very large considering the high solubility and dispersity of amino acids and monosaccharides in water. Additionally, the flow of water changes the water phase interacting with the extraction phase, thus further increasing the bulk concentration-related water volume. In comparison, the grab sampling only represented transient glimpses of the flowing river water by capturing small-volume samples. Therefore, on-site sampling in flowing river water during a 10 min period can reflect a much larger water volume than the grab sampling. Consequently, the spinning sampling technique not only simplified the sampling procedure for the analysis of highly water-soluble organics but also provided results that better indicate the actual concentrations in environmental water.

In light of the feasibility and accuracy demonstrated in the field test, we further applied the spinning sampling technique to monitor the analyte concentrations in the river. The concentrations of the amino acids and monosaccharides in the North Saskatchewan River were measured daily using the spinning sampling technique at the same location over a week. Figure 5 presents the concentrations of the monosaccharides and amino acids in the river. Table S2 summarizes the river water conditions during the week. The concentrations of the monosaccharides and amino acids were found to fluctuate moderately during the monitoring period, and no significant change was observed. The field monitoring was performed during early fall when the weather was calm. These highly water-soluble organics may be present consistently in river water within a short period of time. The concentrations of amino acids Asp, Gln, Met, Phe, Pro, Tyr, and Val were in the

https://doi.org/10.1021/acs.est.2c01202
Environ. Sci. Technol. 2022, 56, 8094−8102

ranges of 2.5−6.7, 3.7−9.7, 2.1−8.5, 14−31, 5.1−18, 10−27, and 6.5−23 ng L^{-1}, respectively, during the monitoring week. For the monosaccharides, Glu was consistently predominant in each sampling with concentrations ranging from 54 to 82 ng L^{-1}, while the concentrations of the other monosaccharides Deo, Gal, Man, Rha, Rib, and Xyl were 2.4−5.2, 9.3−22, 7.2−21, 4.2−12, 5.8−18, and 13−27 ng L^{-1}, respectively. The one-week longitudinal monitoring trial demonstrated the spinning sampling technique for field survey applications.

In this study, we have created a simple method for the preparation of the functionalized NiS-SM disks and a spinning sampling technique of highly soluble natural organics in water. The results of both laboratory and field studies demonstrated the advantages and feasibility of the spinning sampling technique for on-site sampling of trace-level organics in environmental water. This new approach eliminates the need for collection, transport, and storage of large volumes of water samples and enables field studies. Because the spinning sampling technique can rapidly measure the free concentrations in water, it provides the unique capability to study the fate and transport of soluble organics in water systems.[53,54]

■ ASSOCIATED CONTENT

Supporting Information

The Supporting Information is available free of charge at https://pubs.acs.org/doi/10.1021/acs.est.2c01202.

Sample preparation methods, instrument analysis methods, photographs of sampling devices, energy-dispersive spectroscopy mapping images, XPS analysis images, FT-IR analysis images, extraction kinetics figures, sampling rates, and river water conditions (PDF)

■ AUTHOR INFORMATION

Corresponding Author

Xing-Fang Li − *Division of Analytical and Environmental Toxicology, Department of Laboratory Medicine and Pathology, Faculty of Medicine and Dentistry, University of Alberta, Edmonton, Alberta T6G 2G3, Canada;* orcid.org/0000-0003-1844-7700; Phone: 1-780-492-5094; Email: xingfang.li@ualberta.ca

Authors

Junlang Qiu − *School of Environmental Science and Engineering, Sun Yat-sen University, Guangzhou 510006, China; Division of Analytical and Environmental Toxicology, Department of Laboratory Medicine and Pathology, Faculty of Medicine and Dentistry, University of Alberta, Edmonton, Alberta T6G 2G3, Canada*

Caley B. Craven − *Division of Analytical and Environmental Toxicology, Department of Laboratory Medicine and Pathology, Faculty of Medicine and Dentistry, University of Alberta, Edmonton, Alberta T6G 2G3, Canada*

Nicholas J. P. Wawryk − *Division of Analytical and Environmental Toxicology, Department of Laboratory Medicine and Pathology, Faculty of Medicine and Dentistry, University of Alberta, Edmonton, Alberta T6G 2G3, Canada*

Gangfeng Ouyang − *School of Chemistry, Sun Yat-sen University, Guangzhou 510006, China;* orcid.org/0000-0002-0797-6036

Complete contact information is available at: https://pubs.acs.org/10.1021/acs.est.2c01202

Notes

The authors declare no competing financial interest.

■ ACKNOWLEDGMENTS

This project is partially supported by grants from Alberta Innovates, EPCOR, the Natural Sciences and Engineering Research Council of Canada, and the Canada Research Chairs Program.

■ REFERENCES

(1) Hertkorn, N.; Claus, H.; Schmitt-Kopplin, P.; Perdue, E. M.; Filip, Z. Utilization and Transformation of Aquatic Humic Substances by Autochthonous Microorganisms. *Environ. Sci. Technol.* **2002**, *36*, 4334−4345.

(2) Benner, R.; Kaiser, K. Biological and photochemical transformations of amino acids and lignin phenols in riverine dissolved organic matter. *Biogeochemistry* **2011**, *102*, 209−222.

(3) Bertilsson, S.; Tranvik, L. J. Photochemical transformation of dissolved organic matter in lakes. *Limnol. Oceanogr.* **2000**, *45*, 753−762.

(4) Li, X.-F.; Mitch, W. A. Drinking Water Disinfection Byproducts (DBPs) and Human Health Effects: Multidisciplinary Challenges and Opportunities. *Environ. Sci. Technol.* **2018**, *52*, 1681−1689.

(5) Chang, H.; Chen, C.; Wang, G. Identification of potential nitrogenous organic precursors for C-, N-DBPs and characterization of their DBPs formation. *Water Res.* **2011**, *45*, 3753−3764.

(6) Lee, W.; Westerhoff, P.; Croué, J.-P. Dissolved Organic Nitrogen as a Precursor for Chloroform, Dichloroacetonitrile, N-Nitrosodimethylamine, and Trichloronitromethane. *Environ. Sci. Technol.* **2007**, *41*, 5485−5490.

(7) Chu, W.-H.; Gao, N.-Y.; Deng, Y.; Krasner, S. W. Precursors of Dichloroacetamide, an Emerging Nitrogenous DBP Formed during Chlorination or Chloramination. *Environ. Sci. Technol.* **2010**, *44*, 3908−3912.

(8) Huang, G.; Jmaiff Blackstock, L. K.; Jiang, P.; Liu, Z.; Lu, X.; Li, X.-F. Formation, Identification, and Occurrence of New Bromo- and Mixed Halo-Tyrosyl Dipeptides in Chloraminated Water. *Environ. Sci. Technol.* **2019**, *53*, 3672−3680.

(9) Bond, T.; Templeton, M. R.; Graham, N. Precursors of nitrogenous disinfection by-products in drinking water−−A critical review and analysis. *J. Hazard. Mater.* **2012**, *235−236*, 1−16.

(10) Chu, W.; Li, X.; Gao, N.; Deng, Y.; Yin, D.; Li, D.; Chu, T. Peptide bonds affect the formation of haloacetamides, an emerging class of N-DBPs in drinking water: free amino acids versus oligopeptides. *Sci. Rep.* **2015**, *5*, 14412.

(11) Lee, W.; Westerhoff, P. Dissolved organic nitrogen removal during water treatment by aluminum sulfate and cationic polymer coagulation. *Water Res.* **2006**, *40*, 3767−3774.

(12) Huang, G.; Jiang, P.; Jmaiff Blackstock, L. K.; Tian, D.; Li, X.-F. Formation and Occurrence of Iodinated Tyrosyl Dipeptides in Disinfected Drinking Water. *Environ. Sci. Technol.* **2018**, *52*, 4218−4226.

(13) Dotson, A.; Westerhoff, P. Occurrence and removal of amino acids during drinking water treatment. *J. Am. Water Works Assoc.* **2009**, *101*, 101−115.

(14) Shah, A. D.; Mitch, W. A. Halonitroalkanes, Halonitriles, Haloamides, and N-Nitrosamines: A Critical Review of Nitrogenous Disinfection Byproduct Formation Pathways. *Environ. Sci. Technol.* **2012**, *46*, 119−131.

(15) Cai, L.; Li, L.; Yu, S.; Guo, J.; Kuppers, S.; Dong, L. Formation of odorous by-products during chlorination of major amino acids in East Taihu Lake: Impacts of UV, UV/PS and UV/H2O2 pre-treatments. *Water Res.* **2019**, *162*, 427−436.

(16) Navalon, S.; Alvaro, M.; Garcia, H. Carbohydrates as trihalomethanes precursors. Influence of pH and the presence of Cl− and Br− on trihalomethane formation potential. *Water Res.* **2008**, *42*, 3990−4000.

(17) Goslan, E. H.; Seigle, C.; Purcell, D.; Henderson, R.; Parsons, S. A.; Jefferson, B.; Judd, S. J. Carbonaceous and nitrogenous disinfection by-product formation from algal organic matter. *Chemosphere* **2017**, *170*, 1−9.
(18) Poulsen, R.; Cedergreen, N.; Hayes, T.; Hansen, M. Nitrate: An Environmental Endocrine Disruptor? A Review of Evidence and Research Needs. *Environ. Sci. Technol.* **2018**, *52*, 3869−3887.
(19) Vejerano, E. P.; Rao, G.; Khachatryan, L.; Cormier, S. A.; Lomnicki, S. Environmentally Persistent Free Radicals: Insights on a New Class of Pollutants. *Environ. Sci. Technol.* **2018**, *52*, 2468−2481.
(20) Madrid, Y.; Zayas, Z. P. Water sampling: Traditional methods and new approaches in water sampling strategy. *TrAC, Trends Anal. Chem.* **2007**, *26*, 293−299.
(21) Ouyang, G.; Cui, S.; Qin, Z.; Pawliszyn, J. One-Calibrant Kinetic Calibration for On-Site Water Sampling with Solid-Phase Microextraction. *Anal. Chem.* **2009**, *81*, 5629−5636.
(22) Fernandez, L. A.; Lao, W.; Maruya, K. A.; White, C.; Burgess, R. M. Passive Sampling to Measure Baseline Dissolved Persistent Organic Pollutant Concentrations in the Water Column of the Palos Verdes Shelf Superfund Site. *Environ. Sci. Technol.* **2012**, *46*, 11937−11947.
(23) Vrana, B.; Allan, I. J.; Greenwood, R.; Mills, G. A.; Dominiak, E.; Svensson, K.; Knutsson, J.; Morrison, G. Passive sampling techniques for monitoring pollutants in water. *TrAC, Trends Anal. Chem.* **2005**, *24*, 845−868.
(24) Ouyang, G.; Zhao, W.; Bragg, L.; Qin, Z.; Alaee, M.; Pawliszyn, J. Time-Weighted Average Water Sampling in Lake Ontario with Solid-Phase Microextraction Passive Samplers. *Environ. Sci. Technol.* **2007**, *41*, 4026−4031.
(25) Ahmadi, F.; Sparham, C.; Boyacı, E.; Pawliszyn, J. Time Weighted Average Concentration Monitoring Based on Thin Film Solid Phase Microextraction. *Environ. Sci. Technol.* **2017**, *51*, 3929−3937.
(26) Guo, C.; Zhang, T.; Hou, S.; Lv, J.; Zhang, Y.; Wu, F.; Hua, Z.; Meng, W.; Zhang, H.; Xu, J. Investigation and Application of a New Passive Sampling Technique for in Situ Monitoring of Illicit Drugs in Waste Waters and Rivers. *Environ. Sci. Technol.* **2017**, *51*, 9101−9108.
(27) Joyce, A. S.; Portis, L. M.; Parks, A. N.; Burgess, R. M. Evaluating the Relationship between Equilibrium Passive Sampler Uptake and Aquatic Organism Bioaccumulation. *Environ. Sci. Technol.* **2016**, *50*, 11437−11451.
(28) Zeng, E. Y.; Peng, J.; Tsukada, D.; Ku, T.-L. In Situ Measurements of Polychlorinated Biphenyls in the Waters of San Diego Bay, California. *Environ. Sci. Technol.* **2002**, *36*, 4975−4980.
(29) Jonsson, O.; Paulsson, E.; Kreuger, J. TIMFIE Sampler−A New Time-Integrating, Active, Low-Tech Sampling Device for Quantitative Monitoring of Pesticides in Whole Water. *Environ. Sci. Technol.* **2019**, *53*, 279−286.
(30) Lin, K.; Zhang, L.; Li, Q.; Lu, B.; Yu, Y.; Pei, J.; Yuan, D.; Gan, J. A Novel Active Sampler Coupling Osmotic Pump and Solid Phase Extraction for in Situ Sampling of Organic Pollutants in Surface Water. *Environ. Sci. Technol.* **2019**, *53*, 2579−2585.
(31) Roll, I. B.; Halden, R. U. Critical review of factors governing data quality of integrative samplers employed in environmental water monitoring. *Water Res.* **2016**, *94*, 200−207.
(32) Behmel, S.; Damour, M.; Ludwig, R.; Rodriguez, M. J. Water quality monitoring strategies—A review and future perspectives. *Sci. Total Environ.* **2016**, *571*, 1312−1329.
(33) Hureiki, L.; Croué, J. P.; Legube, B. Chlorination studies of free and combined amino acids. *Water Res.* **1994**, *28*, 2521−2531.
(34) Hayakawa, K. Seasonal variations and dynamics of dissolved carbohydrates in Lake Biwa. *Org. Geochem.* **2004**, *35*, 169−179.
(35) Svec, F.; Lv, Y. Advances and Recent Trends in the Field of Monolithic Columns for Chromatography. *Anal. Chem.* **2015**, *87*, 250−273.
(36) Hara, T.; Futagami, S.; De Malsche, W.; Eeltink, S.; Terryn, H.; Baron, G. V.; Desmet, G. Chromatographic Properties of Minimal Aspect Ratio Monolithic Silica Columns. *Anal. Chem.* **2017**, *89*, 10948−10956.
(37) Wu, C.; Liang, Y.; Yang, K.; Min, Y.; Liang, Z.; Zhang, L.; Zhang, Y. Clickable Periodic Mesoporous Organosilica Monolith for Highly Efficient Capillary Chromatographic Separation. *Anal. Chem.* **2016**, *88*, 1521−1525.
(38) Namera, A.; Saito, T. Advances in monolithic materials for sample preparation in drug and pharmaceutical analysis. *Trac. Trends Anal. Chem.* **2013**, *45*, 182−196.
(39) Liu, J.; Wang, F.; Lin, H.; Zhu, J.; Bian, Y.; Cheng, K.; Zou, H. Monolithic Capillary Column Based Glycoproteomic Reactor for High-Sensitive Analysis of N-Glycoproteome. *Anal. Chem.* **2013**, *85*, 2847−2852.
(40) Liu, Z.; Jiang, P.; Huang, G.; Yan, X.; Li, X.-F. Silica Monolith Nested in Sponge (SiMNS): A Composite Monolith as a New Solid Phase Extraction Material for Environmental Analysis. *Anal. Chem.* **2019**, *91*, 3659−3666.
(41) Horie, K.; Kamakura, T.; Ikegami, T.; Wakabayashi, M.; Kato, T.; Tanaka, N.; Ishihama, Y. Hydrophilic Interaction Chromatography Using a Meter-Scale Monolithic Silica Capillary Column for Proteomics LC-MS. *Anal. Chem.* **2014**, *86*, 3817−3824.
(42) Dong, M.; Wu, M.; Wang, F.; Qin, H.; Han, G.; Dong, J.; Wu, R. a.; Ye, M.; Liu, Z.; Zou, H. Coupling Strong Anion-Exchange Monolithic Capillary with MALDI-TOF MS for Sensitive Detection of Phosphopeptides in Protein Digest. *Anal. Chem.* **2010**, *82*, 2907−2915.
(43) Zhang, Z.; Wu, M.; Wu, R. a.; Dong, J.; Ou, J.; Zou, H. Preparation of Perphenylcarbamoylated β-Cyclodextrin-silica Hybrid Monolithic Column with "One-Pot" Approach for Enantioseparation by Capillary Liquid Chromatography. *Anal. Chem.* **2011**, *83*, 3616−3622.
(44) Li, H.; Wang, H.; Liu, Y.; Liu, Z. A benzoboroxole-functionalized monolithic column for the selective enrichment and separation of cis-diol containing biomolecules. *Chem. Commun.* **2012**, *48*, 4115−4117.
(45) Mu, B.; McNicholas, T. P.; Zhang, J.; Hilmer, A. J.; Jin, Z.; Reuel, N. F.; Kim, J.-H.; Yum, K.; Strano, M. S. A Structure−Function Relationship for the Optical Modulation of Phenyl Boronic Acid-Grafted, Polyethylene Glycol-Wrapped Single-Walled Carbon Nanotubes. *J. Am. Chem. Soc.* **2012**, *134*, 17620−17627.
(46) Jin, S.; Cheng, Y.; Reid, S.; Li, M.; Wang, B. Carbohydrate recognition by boronolectins, small molecules, and lectins. *Med. Res. Rev.* **2010**, *30*, 171−257.
(47) Ouyang, G.; Pawliszyn, J. A critical review in calibration methods for solid-phase microextraction. *Anal. Chim. Acta* **2008**, *627*, 184−197.
(48) Murdock, C.; Kelly, M.; Chang, L.-Y.; Davison, W.; Zhang, H. DGT as an in Situ Tool for Measuring Radiocesium in Natural Waters. *Environ. Sci. Technol.* **2001**, *35*, 4530−4535.
(49) Huckins, J. N.; Petty, J. D.; Orazio, C. E.; Lebo, J. A.; Clark, R. C.; Gibson, V. L.; Gala, W. R.; Echols, K. R. Determination of Uptake Kinetics (Sampling Rates) by Lipid-Containing Semipermeable Membrane Devices (SPMDs) for Polycyclic Aromatic Hydrocarbons (PAHs) in Water. *Environ. Sci. Technol.* **1999**, *33*, 3918−3923.
(50) Chen, Y.; Koziel, J. A.; Pawliszyn, J. Calibration for On-Site Analysis of Hydrocarbons in Aqueous and Gaseous Samples Using Solid-Phase Microextraction. *Anal. Chem.* **2003**, *75*, 6485−6493.
(51) Sukola, K.; Koziel, J.; Augusto, F.; Pawliszyn, J. Diffusion-Based Calibration for SPME Analysis of Aqueous Samples. *Anal. Chem.* **2001**, *73*, 13−18.
(52) Qin, Z.; Bragg, L.; Ouyang, G.; Niri, V. H.; Pawliszyn, J. Solid-phase microextraction under controlled agitation conditions for rapid on-site sampling of organic pollutants in water. *J. Chromatogr. A* **2009**, *1216*, 6979−6985.
(53) Bondarenko, S.; Gan, J. Simultaneous Measurement of Free and Total Concentrations of Hydrophobic Compounds. *Environ. Sci. Technol.* **2009**, *43*, 3772−3777.
(54) Cui, X.; Bao, L.; Gan, J. Solid-phase Microextraction (SPME) with Stable Isotope Calibration for Measuring Bioavailability of Hydrophobic Organic Contaminants. *Environ. Sci. Technol.* **2013**, *47*, 9833−9840.

https://doi.org/10.1021/acs.est.2c01202
Environ. Sci. Technol. 2022, 56, 8094−8102